

Analysis of Aerodynamics Load of a Flapping Wing by Vortex Lattice Method

¹Ismoyo Haryanto, ^{2*}Khoiri Rozi, ³Berkah Fajar TK, ⁴Alwahidil Zuhri

^{1,2,3,4}Mechanical Engineering, Diponegoro University, Jl. Prof. H. Soedarto, SH, Tembalang, Semarang 50275, Indonesia

*Corresponding Author's E-mail: khoiri.rozi@yahoo.com

Abstract - The aim of this study is to investigate the effect of changing the angle of attack and flapping angle on the aerodynamic characteristics of an unsymmetrical wing with the NACA 2412 profile. This work uses the Vortex Lattice Method. The results of this study show that increasing the flapping angle causes the pitching moment to decrease while induced drag and moment coefficient increase, meanwhile, the lift coefficient increases at positive angles of attack and then decreases at negative angles of attack. The pitching moment decreases with increasing angle of attack at positive flap angles, but this value increases at negative flap angles. Meanwhile, the induced drag decreases from an angle of attack -15° to a minimum at an angle of attack -5° and then increases. The moment coefficient increases with increasing angle of attack at positive flapping angles, but decreases at negative flapping angles. Meanwhile, the lift coefficient increases with increasing angle of attack.

Keywords: aerodynamic characteristic, angle of attack, flapping wing, flapping angle.

I. INTRODUCTION

Currently, the concept of flying with a flapping-wing is often found with a micro aerial vehicle (MAV) which becomes a flapping-wing micro aerial vehicle (FWMAV). This concept design was first introduced by Leonardo da Vinci in the 15th century [1]. This breakthrough is an optimization of flight mechanisms by imitating concepts that exist in nature with a relatively small size [2]. Animals such as birds and insects can fly with extraordinary aerodynamic performance, using only wing beats and special mechanisms [3]. This mechanism has become an inspiration for the development of more innovative aviation technology [4].

One of the important foundations of this research is the concept of biomimetics, where the FWMAV design modeling replicates the concept of flight that exists in animals, especially birds. To improve the performance of FWMAV it is necessary to understand how to optimize the movement of the wing flaps [5]. By understanding how animal wings produce aerodynamic aspects that support flight, FWMAVs can be developed that are able to overcome air resistance and produce

better lift [6]. Therefore, along with the development of research related to this mechanism, it will bring a better and more efficient world of aeromodelling [7].

Understanding the aerodynamic aspects of flapping wings allows the design of small aircraft that can operate efficiently and stably in various environments [8]. This is highly relevant in various sectors, including surveillance, mapping, and military [9].

By referring to the basics above, this research was carried out which examined the effect of changes in flap angle and angle of attack on the aerodynamic characteristics of aircraft. The method used in this study uses the vortex lattice method with the NACA 2412 wing profile test model.

II. METHODOLOGY

2.1 Wing Model

This research uses a wing model as shown in Figure 1 with a NACA 2412 unsymmetrical airfoil profile as shown in Figure 2. The NACA 2412 airfoil has a maximum chamber of 2% which is located at 40% of the chord from the leading edge and has a maximum thickness of 12% of the chord length (0.12C).

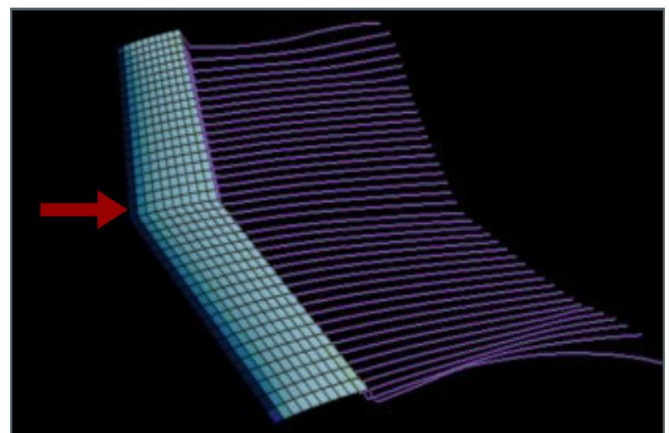


Figure 1: Wing Model Test

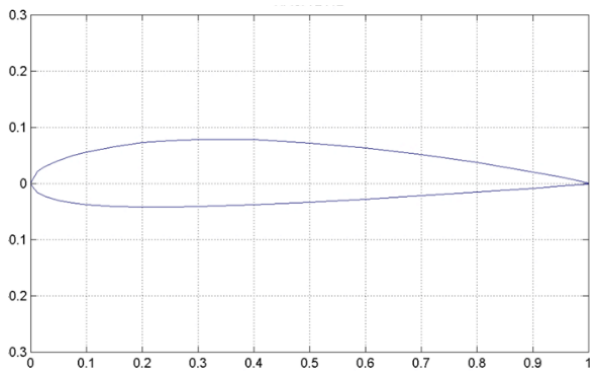


Figure 2: Airfoil NACA 2412

2.2 Vortex Lattice Method (VLM)

The Vortex-Lattice Method is an aerodynamic simulation method used to analyze and model aerodynamic force loads on aircraft wings using the Laplace approach [10]. An illustration of this VLM approach is shown in Figure 3 below.

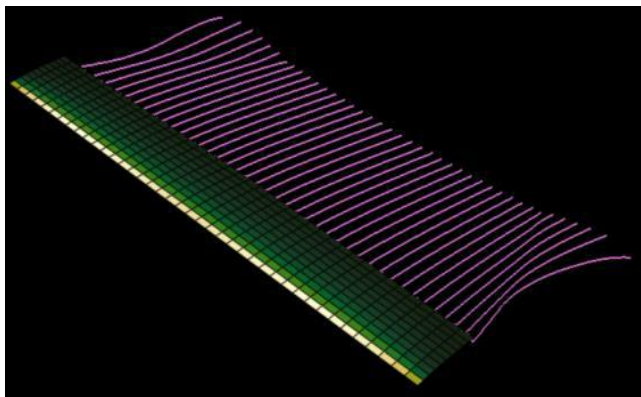


Figure 3: Vortex Lattice Method [11]

2.3 Parameters

In this study, the effect of changing the angle of attack on the aerodynamic characteristics of the wing with several changes in the wing flap angle was tested. Variations in the angle of attack tested were at $\alpha = -15^\circ, -10^\circ, -5^\circ, 0^\circ, 5^\circ, 10^\circ, 15^\circ$ with the definition of the angle of attack illustrated in Figure 4. Meanwhile, the definition of variations in positive and negative wing flap angles $\theta = -60^\circ, -40^\circ, -20^\circ, 0^\circ, 20^\circ, 40^\circ, 60^\circ$ are illustrated by Figure 5.

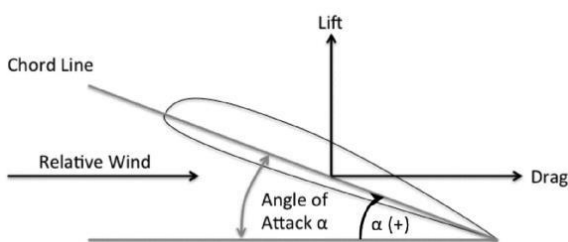


Figure 4: Angle of attack definition

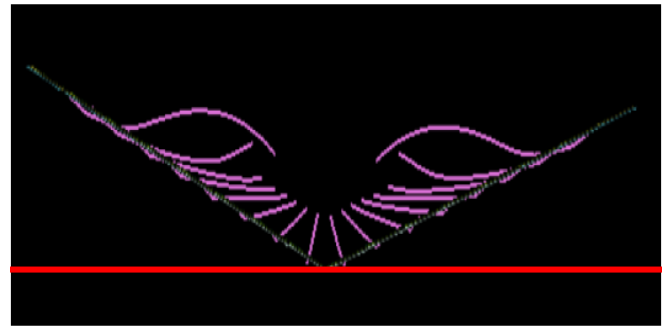


Figure 5: Flapping angle of wing at 20°

2.4 Validation

In this study, the simulation results were compared with research conducted by Nguyen [12]. This research aims to analyze the distribution of lift and drag on the wing surface with varying test speeds from 0 to 50 m/s. This research was used as validation. A comparison between simulations can be seen in Figure 6 below.

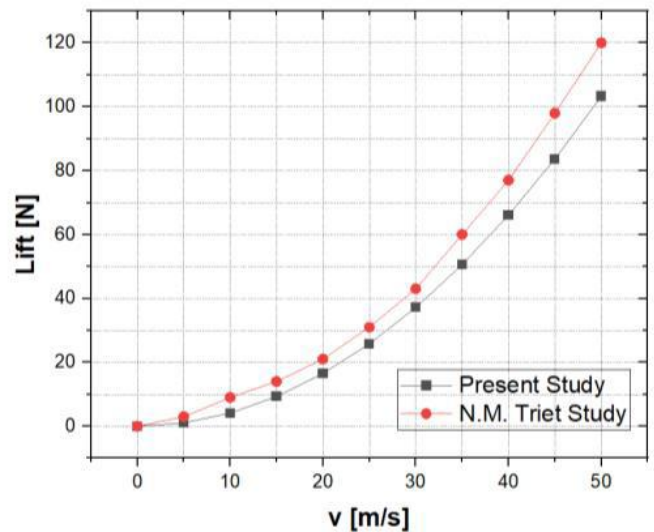


Figure 6: Comparison simulation (present) and work of Nguyen [12]

III. RESULTS AND DISCUSSIONS

3.1 Lift coefficient (C_L)

The simulation results of the lift coefficient as a function of angle of attack at several variations of positive and negative flap angles are plotted in Figures 7 and 8. For positive flap angles ($\theta = 20^\circ, 40^\circ, 60^\circ$) as seen in Figure 7, it can be seen that the values C_L increases as the angle of attack variation increases, with a maximum lift value of $\alpha = 15^\circ$ at a flap angle of $\theta = 20^\circ$. The trend of increasing C_L has a similar pattern at each variation of flap angle. Increasing the angle of attack makes the C_L value higher and the upward trend becomes sharper.

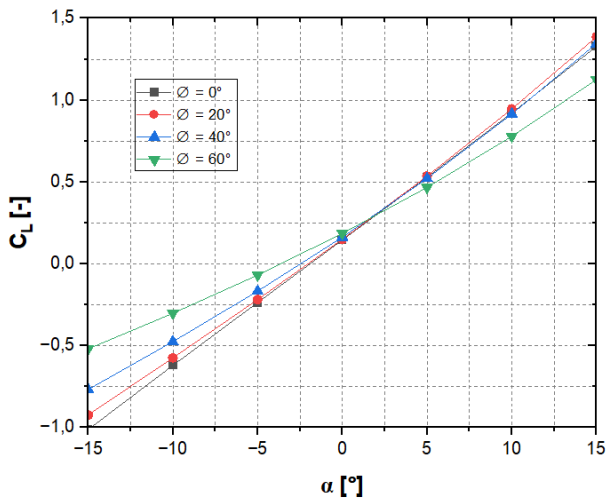


Figure 7: Lift coefficient as a function of angle of attack at positive flapping angle

For negative strike angles ($\theta = -20^\circ, -40^\circ, -60^\circ$) as shown in Figure 8, from this it can be found that the C_L value increases with increasing angle of attack up to the maximum point, with the lowest value at $\alpha = -15^\circ$ at flap angle $\alpha = -20^\circ$. Increasing the angle of attack causes the resulting C_L value to increase. In general, the two plots show that variations in positive and negative angles of attack have almost the same trend pattern of increasing C_L .

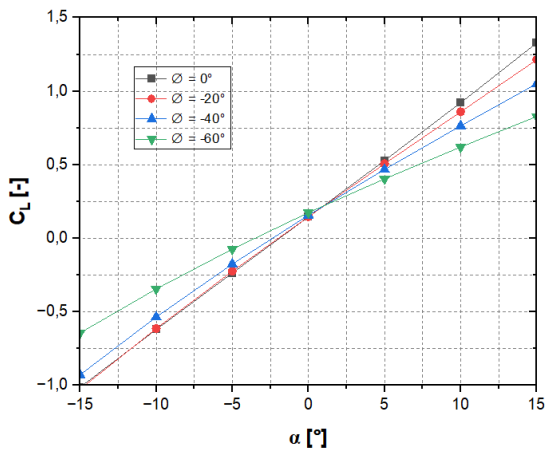


Figure 8: Lift coefficient as a function of angle of attack at negative flapping angle

3.2 Induced drag coefficient (CDi)

Figures 9 and 10 are the simulation results of the induced drag coefficient as a function of the angle of attack at positive flap angles ($\theta = 20^\circ, 40^\circ, 60^\circ$) and negative flap angles ($\theta = -20^\circ, -40^\circ, -60^\circ$). For positive flap angles as shown in Figure 9, it can be found that the highest CD_i is at an angle of attack $\alpha = 15^\circ$ and a flap angle of $\theta = -60^\circ$. It can also be seen that the CD_i value tends to decrease from a negative angle of attack to the minimum point at an angle of attack $\alpha = -5^\circ$ which then increases as the angle of attack value increases.

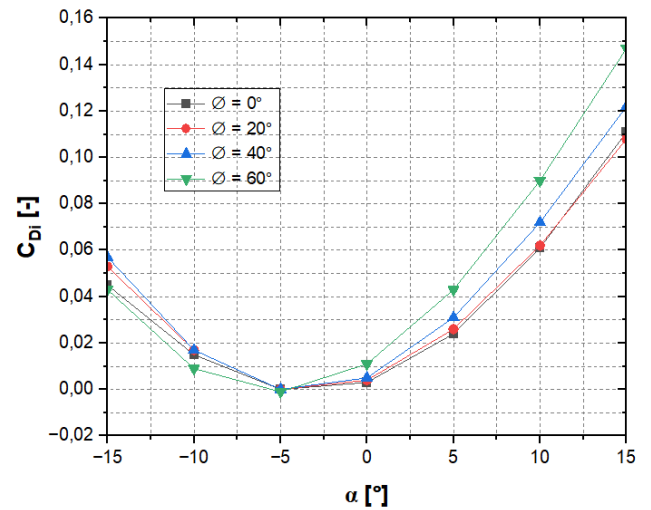


Figure 9: Induced drag as a function of angle of attack at positive flapping angle

At a negative angle of attack as presented in Figure 10, it can be seen that the CD_i value moves down from a negative angle of attack to the minimum point at an angle of attack of $\alpha = -5^\circ$, which then moves to increase significantly along with the increase in the value of the angle of attack tested. The highest CD_i is seen at an angle of attack of $\alpha = 15^\circ$ and a flap angle of $\theta = -60^\circ$. This generally applies to all flap angles tested as can be seen in the plots of the simulation results that have been carried out.

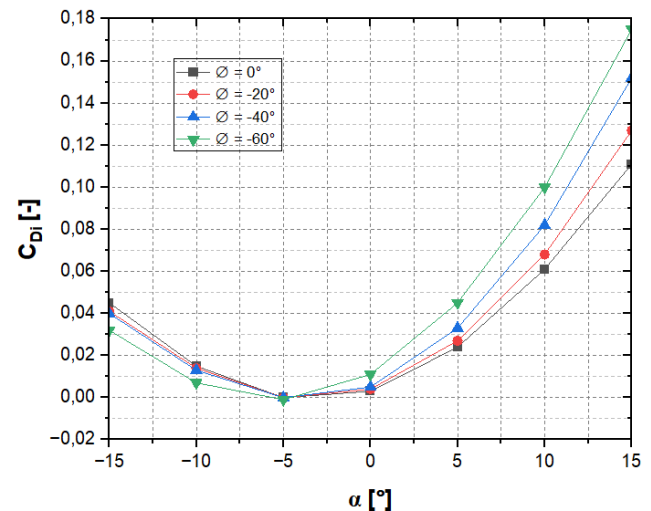


Figure 10: Induced drag as a function of angle of attack at positive flapping angle

3.3 Pitching Moment

Pitching moment simulation results as a function of angle of attack at several variations of positive ($\theta = 20^\circ, 40^\circ, 60^\circ$) and negative ($\theta = -20^\circ, -40^\circ, -60^\circ$) flap angles are plotted in Figures 11 and 12. For the positive pitch angle as shown in Figure 11 can be noted that the pitching moment tends to

increase to a maximum point at an angle of attack $\alpha = -5^\circ$ and then decreases as the angle of attack increases. The lowest pitching moment value is located at an attack angle of $\alpha = 15^\circ$ and a flapping angle of $\theta = 60^\circ$. From the picture it can also be seen that the trend in each test variation has the same movement pattern.

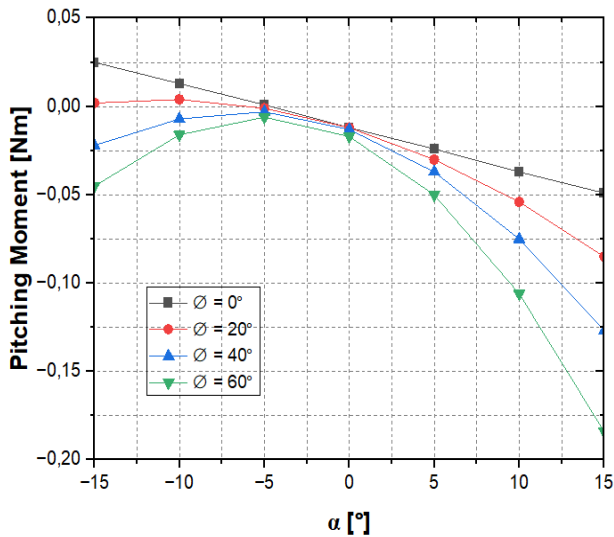


Figure 11: Pitching moment as a function of angle of attack at positive flapping angle

For a negative flap angle as shown in Figure 12, it can be seen that the pitching moment moves down to a minimum point at an angle of attack $\alpha = 0^\circ$ and then moves up as the value of the angle of attack increases. It is also known that the highest point is achieved at varying angles of attack $\alpha = -15^\circ$ and flap angles $\theta = 0^\circ$. While the lowest point is achieved at attack variations of $\alpha = 15^\circ$ and flapping angle of $\theta = 60^\circ$.

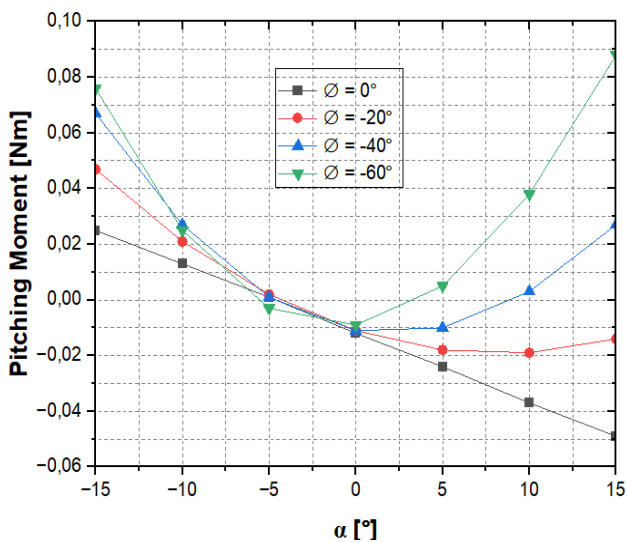


Figure 12: Pitching moment as a function of angle of attack at negative flapping angle

3.4 Moment coefficient (Cm)

The simulation results of the moment coefficient as a function of angle of attack at various positive ($\theta = 20^\circ, 40^\circ, 60^\circ$) and negative ($\theta = -20^\circ, -40^\circ, -60^\circ$) stroke angles are shown in Figures 13 and 14. For positive flap angle as shown in Figure 13. It can be seen that the moment coefficient value moves down to the minimum point at the angle of attack $\alpha = -5^\circ$ and then moves up as the angle of attack increases. From the graph it can be seen that the Cm value is highest in the test variation of angle of attack $\alpha = 15^\circ$ and flapping angle $\theta = 60^\circ$. In general, from the plot it is also found that the trend in each test variation has the same movement pattern.

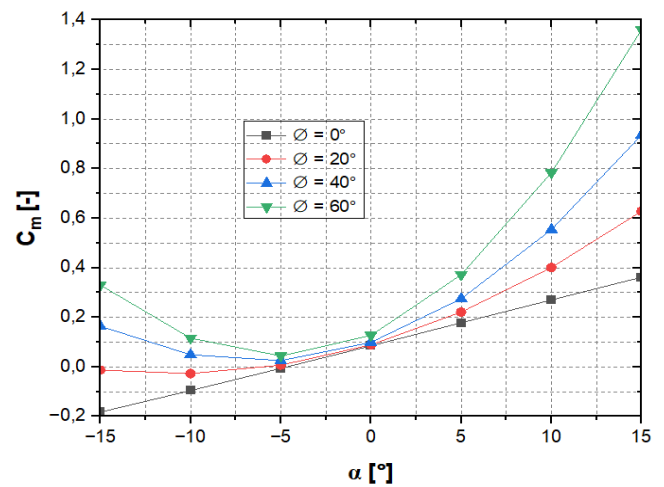


Figure 13: Moment coefficient as a function of angle of attack at positive flapping angle

For negative flap angles as shown in Figure 14, it can be seen that the moment coefficient moves up to a maximum point at angles of attack $\alpha = 0^\circ$ and $\alpha = 5^\circ$, which then decreases significantly as the angle of attack increases. It can also be seen that the Cm value is lowest in the test variation of angle of attack $\alpha = -15^\circ$ and flapping angle $\theta = -60^\circ$.

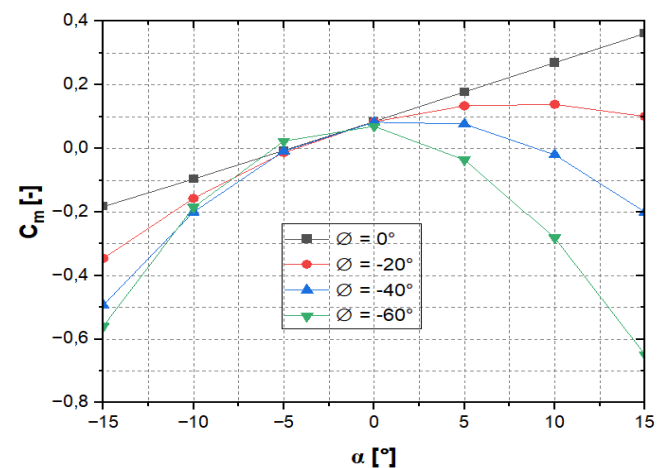


Figure 14: Moment coefficient as a function of angle of attack at negative flapping angle

IV. CONCLUSION

Several important results from this research can be summarized as follows: increasing the flap angle causes the pitching moment to decrease while the induced drag and moment coefficient increase, while C_L increases at positive angles of attack and then decreases at negative angles of attack. The value of pitching moment decreases with increasing angle of attack at a positive angle of attack but this value increases at a negative angle of attack. Meanwhile the value of induced drag decreases from an angle of attack -15° to a minimum at an angle of attack -5° , then increases. The moment coefficient increases with increasing angle of attack at positive flapping angles, but decreases at negative flapping angles. Meanwhile, the lift coefficient value increases with increasing angle of attack.

REFERENCES

- [1] A.J. Singh, S. Wala, S. H. Ladakhan, R. B. Sreesh, and S. M. Adinarayanappa, "Design and fabrication of shape memory alloy based 4D-printed actuator for FWMAV: A performance study," *Mater. Today Proc.*, no. xxxx, 2023.
- [2] T. Ozaki and K. Hamaguchi, "Improved lift force of a resonant-driven flapping-wing micro aerial vehicle by suppressing wing-body and wing-wing vibration coupling," *Extrem. Mech. Lett.*, vol. 40, p. 100867, 2020.
- [3] T. Q. Le, J. H. Ko, D. Byun, S. H. Park, and H. C. Park, "Effect of Chord Flexure on Aerodynamic Performance of a Flapping Wing," *J. Bionic Eng.*, vol. 7, no. 1, pp. 87–94, 2010.
- [4] W. He, X. Mu, L. Zhang, and Y. Zou, "Modeling and trajectory tracking control for flapping-wing micro aerial vehicles," *IEEE/CAA J. Autom. Sin.*, vol. 8, no. 1, pp. 148–156, 2021.
- [5] T. WANG, L. LIU, J. LI, and L. ZENG, "Time-history performance optimization of flapping wing motion using a deep learning based prediction model," *Chinese J. Aeronaut.*, vol. 37, no. 5, pp. 317–331, 2024.
- [6] M. Kiani et al., "A new bio-inspired flying concept: The quad-flapper," *AIAA Scitech 2019 Forum*, no. January, pp. 1–12, 2019.
- [7] M. F. Bin Abas, A. S. Bin Mohd Rafie, H. Bin Yusoff, and K. A. Bin Ahmad, "Flapping wing micro-aerial vehicle: Kinematics, membranes, and flapping mechanisms of ornithopter and insect flight," *Chinese J. Aeronaut.*, vol. 29, no. 5, pp. 1159–1177, 2016.
- [8] F. Song, Y. Yan, and J. Sun, "Review of insect-inspired wing micro air vehicle," *Arthropod Struct. Dev.*, vol. 72, p. 101225, 2023.
- [9] S. Xiao, K. Hu, B. Huang, H. Deng, and X. Ding, "A Review of Research on the Mechanical Design of Hoverable Flapping Wing Micro-Air Vehicles," *J. Bionic Eng.*, vol. 18, no. 6, pp. 1235–1254, 2021.
- [10] D. Livescu, "Applied Computational Aerodynamics. A Modern Engineering Approach," *AIAA J.*, vol. 54, no. 11, pp. 3679–3680, 2016.
- [11] J. D. Anderson, *Fundamentals of Aerodynamics (6th edition)*, vol. 1984, no. 3. 2011.
- [12] M. T. Nguyen, N. V. Nguyen, and M. T. Pham, "Aerodynamic Analysis of Aircraft Wing," *VNU J. Sci. Math. – Phys.*, vol. 31, no. 2, pp. 68–75, 2015.

Citation of this Article:

Ismoyo Haryanto, Khoiri Rozi, Berkah Fajar TK, & Alwahidil Zuhri. (2024). Analysis of Aerodynamics Load of a Flapping Wing by Vortex Lattice Method. *International Research Journal of Innovations in Engineering and Technology - IRJIET*, 8(9), 297-301. Article DOI <https://doi.org/10.47001/IRJIET/2024.809036>
